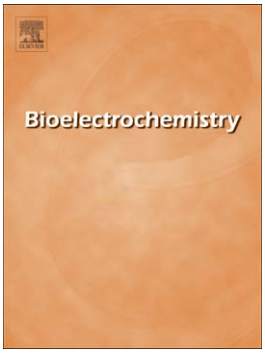


# Electrochemical study of quinone redox cycling: A novel application of DNA-based biosensors for monitoring biochemical reactions

Ali A. Ensafi, Hamid Reza Jamei, Esmaeil Heydari-Bafrooei, B. Rezaei

PII: S1567-5394(16)30060-3
DOI: doi: 10.1016/j.bioelechem.2016.04.008
Reference: BIOJEC 6943

To appear in: *Bioelectrochemistry*

Received date: 8 April 2016
Revised date: 26 April 2016
Accepted date: 26 April 2016

Please cite this article as: Ali A. Ensafi, Hamid Reza Jamei, Esmaeil Heydari-Bafrooei, B. Rezaei, Electrochemical study of quinone redox cycling: A novel application of DNA-based biosensors for monitoring biochemical reactions, *Bioelectrochemistry* (2016), doi: 10.1016/j.bioelechem.2016.04.008

# Electrochemical study of quinone redox cycling: a novel application of DNA-based biosensors for monitoring biochemical reactions

**Ali A. Ensafi[a,*], Hamid Reza Jamei[a], Esmaeil Heydari-Bafrooei[b], B. Rezaei[a]**

[a] *Department of Analytical Chemistry, College of Chemistry, Isfahan University of Technology, Isfahan 84156–83111, Iran*

[b] *Department of Chemistry, Faculty of Science, Vali-e-Asr University, Rafsanjan 77188–97111, Iran*

**Abstract**

This paper presents the results of an experimental investigation of voltammetric and impedimetric DNA-based biosensors for monitoring biological and chemical redox cycling reactions involving free radical intermediates. The concept is based on associating the amounts of radicals generated with the electrochemical signals produced, using differential pulse voltammetry (DPV) and electrochemical impedance spectroscopy (EIS). For this purpose, a pencil graphite electrode (PGE) modified with multiwall carbon nanotubes and poly-diallydimethlammonium chloride decorated with double stranded fish sperm DNA was prepared to detect DNA damage induced by the radicals generated from a redox cycling quinone (i.e., menadione (MD; 2-methyl-1,4-naphthoquinone)). Menadione was employed as a model compound to study the redox cycling of quinones. A direct relationship was found between free radical production and DNA damage. The relationship between MD-induced DNA damage and free radical generation was investigated in an attempt to identify the possible mechanism(s) involved in the action of MD. Results showed that DPV and EIS were appropriate, simple and inexpensive techniques for the quantitative and qualitative

* Correspondence address: Tel.: +98–31–33912351; Fax: +98–31–33912350. E–mail: ensafi@cc.iut.ac.ir; aaensafi@gmail.com

comparisons of different reducing reagents. These techniques may be recommended for monitoring DNA damages and investigating the mechanisms involved in the production of redox cycling compounds.

**Keywords:** Quinone redox cycling; Menadione; DNA-based biosensor; Electrochemical impedance spectroscopy.

## 1. Introduction

Quinones form a class of aromatic compounds, which may be called diketones as they include two carbonyl groups in the same or different rings. These compounds play a variety of roles in living organisms, and as such they occur widely in the animal kingdom and extensively in higher plants, fungi (including lichens) and bacteria [1]. They are used as therapeutic agents; as in adriamycin and mitomycin C for cancer chemotherapy. However, they have toxic effects on living organisms as demonstrated by the magnitude of their toxicity to isolated hepatocytes of 5-hydroxy-l,4-naphthoquinone, which is higher than that of 2-hydroxy-l,4-naphthoquinone [2]. Their critical functions in living organisms have encouraged a considerable body of chemical and biochemical research into their properties and behavior [3,4].

Quinone redox cycling is a fundamental process that has been shown to take place in numerous biological systems. In this process, a quinone (Q) is reduced to a semiquinone ($Q^{\cdot-}$) or a hydroquinone ($QH_2$) (Scheme 1). In the presence of $O_2$, $Q^{\cdot-}$ and $QH_2$ are autoxidized to transform quinone, while $O_2$ is reduced to a superoxide anion radical ($O_2^{\cdot-}$), which is a potentially toxic species [4,5]. Most semiquinone radicals react quickly with $O_2$ to generate $O_2^{\cdot-}$; therefore, the one–electron reduction of quinones to semiquinones and the following autoxidation of the semiquinones to quinones may yield large amounts of $O_2^{\cdot-}$. The

generation of $O_2^{\cdot -}$ marks the onset of a cascade of reactions that lead to generation of hydrogen peroxide ($H_2O_2$) and hydroxyl radicals ($OH^{\cdot}$), collectively referred to as "reactive oxygen species" (ROS) [6]. This nonstoichiometric redox process is identified as redox cycling and is responsible for the oxidative damage associated with quinone [1]. The redox chemistry and the biochemistry of quinones have been the subject of much research [6–9].

Quinone redox cycling can be catalyzed by flavoenzymes in living organisms using NADPH as an electron donor. NADPH-cytochrome P450 reductase, NADH-ubiquinone oxidoreductase and NADH-cytochrome $b_5$ reductase are some of the enzymes that catalyze the single-electron reduction while NAD(P)H quinone acceptor oxidoreductase serves as the catalyst for the two-electron reduction [10,11]. Many quinones may also be reduced directly by some electron carriers such as vitamin C (VC) or glutathione [12,13]. For example, naphthoquinones reacting with GSH (reduced glutathione) generate GSH conjugates to form superoxide and hydrogen peroxides [1,14]. Thus, one-electron reduction of quinones to semiquinone radicals by an enzymatic or nonenzymatic mechanism usually leads to the formation of $O_2^{\cdot -}$ and other reactive oxygen species (ROS) [15].

ROSs thus formed engage these compounds in all the oxidative stress-related phenomena in the cell such as signal transduction, gene activation and DNA damage [1,10,16]. A major target of ROS are the electron-rich bases of DNA in the living cells, which undergo oxidation to produce a wide range of genotoxic modifications [17,18].

Electrochemical methods have revealed their considerable advantages in the fast response detection of DNA damage at a relatively low cost and low power consumption [19,20]. The three commonly used electrochemical methods to detect radical-mediated DNA damage are based on either direct oxidation signals of guanine and adenine moiety [18,21], indirect electrochemical indicators [22,23], or impedance signals of modified electrodes [23–25]. In this work, an electroanalytical method was used to fabricate DNA-functionalized biosensors

to investigate the quinone redox cycling. ROS generated by the redox cycling process was observed to induce damages in the surface-confined DNA and, consequently, to change the electrochemical signals. Differential pulse voltammetry (DPV) and electrochemical impedance spectroscopy were then employed to detect DNA damage. Redox cycling of menadione (MD, 2-methylnaphthalene-1,4-dione) was used as a model reaction since MD serves as a good model for investigating the role of quinone moiety in DNA damages due to redox cycling. There are many similar redox cycling compounds whose mechanisms may also be studied using the proposed biosensor. To the best of our knowledge, no previous work has been reported on designing an electrochemical biosensor for investigating redox cycling. Accordingly, it is essential to fabricate appropriate electrode materials that can be used in designing electrochemical biosensors to detect redox cycling and that can serve as an *in vitro* model to simulate the pathway of redox cycling in chemical processes. In this study, poly-diallydimethlammonium chloride (PDDA) was used as a dispersant for MWCNT so that MWCNT-PDDA could be immobilized on the surface of an electrochemically pretreated pencil graphite electrode (PGE) to enhance the electron transfer properties of the electrode surface. Finally, the dsDNA was immobilized at the surface of the MWCNT-PDDA/PGE thus obtained.

## 2. Materials and Methods

### *2.1. Apparatus*

Differential pulse voltammetry (DPV) was performed using an AUTOLAB PGSTAT 12 controlled by a GPES software, version 4.9 (Eco Chemie, The Netherlands). A conventional three-electrode cell (Metrohm Model 663 VA stand) was used, which included a renewable modified-PGE as the working electrode, a platinum wire $5\times10^{-4}$ m in thickness with an exposed end of $10^{-2}$ m as the counter electrode and an Ag|AgCl|$KCl_{sat}$ used as the reference

electrode. A pencil holder (Model DM7-300, Zebra Drafix, Japan) was used to hold the graphite lead (Pentel HB model, 0.7 mm in diameter). Electrical contact was made by soldering a copper wire to the metal part holding the lead inside the pencil. The pencil was then fixed vertically so that a length of 12 mm of the lead would be protruding (and 9 mm would be immersed in the detection solution).

DPV was performed on both damaged and undamaged DNA modified PGEs in an acetate buffer solution containing 0.02 mol $L^{-1}$ NaCl (pH 4.8) free of MD and any other reagents at voltages between +0.40 and +1.40 V *vs.* Ag/AgCl. The operating conditions for DPV studies consisted of: a step potential of 8.0 mV; a modulation amplitude of 50.0 mV; a modulation time of 0.05 s and an interval time equal to 0.5 s. The raw voltammograms of the DPV technique were used after treatment with a Savitzky and Golay filter (level 2) of the GPES software. Average baseline correction was defined as recommended in the relevant literature [26] using a peak width of 0.01 V.

Electrochemical impedance spectroscopy (EIS) measurements were conducted in a three-electrode cell assembly containing an aqueous solution of 5.0 mmol $L^{-1}$ $K_3[Fe(CN)_6]/K_4[Fe(CN)_6]$ (1:1) mixture as a redox probe and 0.1 mol $L^{-1}$ KCl. The EIS was performed from 5 mHz to 100 kHz with the AC amplitude set at 10 mV and a DC potential of +0.25 V *vs.* Ag/AgCl (sat. KCl). Measurements were performed using an AUTOLAB PGSTAT12 with a FRA2 module, version 4.9 (Eco Chemie, The Netherlands). The experimental spectra, presented as Nyquist plots, were fitted with proper equivalent circuits using the software supplied with the instrument.

A pH-meter, Model 827 (Metrohm), combined with a glass electrode–reference electrode was used to control solution pH with an accuracy of ±0.05.

*2.2. Chemicals*

Double-stranded fish sperm DNA (dsDNA) was purchased from Sigma (St. Louis, USA). Stock solution of dsDNA (1000 μg $mL^{-1}$) was prepared with Tris–EDTA buffer (TE buffer; 10 mmol $L^{-1}$ Tris–HCl, 1.0 mmol $L^{-1}$ EDTA, pH 7.0) and kept at –20 °C. A further diluted solution of dsDNA was prepared using 0.5 mol $L^{-1}$ of acetate buffer (pH 4.8) containing 0.02 mol $L^{-1}$ NaCl. Stock solution of MD (1.0 mmol $L^{-1}$), Fluka, was prepared by dissolving accurately weighed amounts of MD in ethanol. More diluted solutions of MD were prepared using a phosphate buffer solution (PBS, pH 7.0). PDDA (low molecular weight) was purchased from Sigma. Aqueous solutions of PDDA were initially prepared using 0.02 mol $L^{-1}$ NaCl. Reagent grade Tris–HCl, $CH_3COOH$, $CH_3COONa$, EDTA, NaCl and NaOH were purchased from Aldrich Chemicals (Milwaukee, USA).

MWCNTs (bundles 70–110 nm in diameter and 5–9 μm in length) were purchased from Aldrich Chemicals (Milwaukee, USA) and activated by heating at reflux in $HNO_3$. For this purpose, 0.50 g of the as-received MWCNTs was sonicated with 40 mL of nitric acid (5.0 mol $L^{-1}$) and refluxed for 20 h. The resulting purified MWCNTs were separated by centrifugation at 4000 rpm for 15 min, washed with 25 mL of water and centrifuged for 15 min. This procedure was repeated until the water layer would exhibit a neutral pH. The activated MWCNTs were then dried under vacuum at room temperature. This procedure induced a substantial damage to carbon nanotubes and introduced –COOH groups into the nanotube structure.

*2.3. Assay procedure*

Unless otherwise stated, all the experiments consisted of the following four steps:

(I) *Pretreatment of the electrode:* A constant potential of +1.40 V, *vs.* Ag/AgCl, was applied to the PGE for 300 s in an acetate buffer solution at pH 4.8. Such a high potential applied in an acidic medium led to improved hydrophilic properties of the electrode surface as a result of introducing oxygenated functionalities.

(II) *Adsorption of MWCNTs*: The pretreated PGEs were immersed for 120 min in 2.0 mg of activated MWCNTs and sonicated for 3 h with 1.0 mL of a solution containing 0.0010 g PDDA and 0.5 mol $L^{-1}$ NaCl. The PGEs were then washed with water and dried in an $N_2$ stream.

(III) *Adsorption of DNA:* PDDA–MWCNT/PGEs were immersed in 1.0 g $L^{-1}$ of the dsDNA, pH 7.0, which had been stirred and buffered with Tris-EDTA for 30 min. The substrates were then rinsed with the acetate buffer (0.5 mol $L^{-1}$ at pH 4.8) and dried in an $N_2$ stream. This modified PGE was designated as the dsDNA/PDDA–MWCNT/PGE.

(IV) *Effect of MD on the surface confined DNA:* The sensor was incubated in the MD solution in both the presence and absence of other reagents in 0.1 mol $L^{-1}$ PBS for a given time under stirring and finally rinsed with water. Then, the sensor was placed in an electrochemical cell containing an appropriate supporting electrolyte, as described in the Apparatus Section, to record the voltammetric and impedimetric responses. The differences in the voltammetric and impedimetric signals obtained from dsDNA/PDDA–MWCNT/PGEs before and after interaction with MD were used as analytical signals. Iterative experiments were performed by renewing the PGE according to the procedure described above.

## 3. Results and discussion

Previous studies by our research group [19,21,24] and those reported elsewhere [27] indicate that PDDA is a particularly stable immobilization agent for DNA and a dispersing agent for MWCNTs. PDDA is a cationic polymer with a good biocompatibility and a high positive charge density that makes it convenient for electrostatic DNA immobilization while it can be used for preparing a stable and sensitive modifier layer at the PGE surface. Anodization of carbon-based electrodes employed in acidic media at high positive potentials increases the surface quinone and other functional groups [28].

MWCNT–PDDA nanocomposites with positive charges could be adsorbed onto the PG surface by both electrostatic and hydrophobic interactions. Negatively charged DNA could then be adsorbed onto the positively charged MWCNT–PDDA modified electrode via the electrostatic attraction between them to form DNA/MWCNT–PDDA films. MWCNTs on the surface of PGEs greatly improves the extent of adsorption and electrooxidation of DNA. Figure 1 shows SEM images of (A) the pretreated PGE, (B) the PGE modified with PDDA–MWCNTs dispersion (PDDA–MWCNT/PGE) and (C) dsDNA/PDDA–MWCNT/PGE. Figure 1A clearly depicts both the surface roughness of the unmodified PGE and the graphite layers. In the SEM image of PDDA–MWCNT/PGE (Figure 1B), MWCNTs are shown to be dispersed in the porous structure of the PDDA matrix with portions of the PGE becoming invisible due to the immobilization of PDDA on the substrate. The SEM image in Figure 1C shows change in the surface morphology and enhancement in surface roughness because of the dsDNA immobilization. Clearly, the PDDA established a polymer backbone on the surface of the electrode enabling firm and homogeneous films. **"Here Figure 1"**

EIS is a major tool for the characterization of films on conductive surfaces [29–32]. In this study, the Nyquist plots of EIS for different electrodes were prepared using 5.0 mmol $L^{-1}$ $K_3[Fe(CN)_6]/K_4[Fe(CN)_6]$ (1:1) solution as an electrochemical probe (Figure 2). The data fitted well with an equivalent circuit (Figure 2, inset). This circuit included the resistive and capacitive elements, in which $R_s$ represents the electrolyte resistance, the constant phase element $Q_1$ is then related to the space charge capacitance at dsDNA/PDDA–MWCNT/electrolyte interface. $R_{ct}$ denotes the charge transfer resistance at dsDNA/PDDA–MWCNT/electrolyte interface and the constant phase element $Q_2$ is the Warburg impedance resulting from the diffusion of ions from the bulk of the electrolyte to the interface.

The impedance of the constant phase element can be expressed as $Z_Q = (j\omega)^{-n}/Y_0$, where, $Y_0$ is the modulus; $\omega$, the angular phase; and n is the phase ($0 \leq n \leq 1$). The constant phase

element exhibits the inhomogeneous and defective areas of the layer. $Y_0$ is the constant of proportionality containing the diffusion coefficient and other parameters which depend on the characteristics of the electrochemical system, $j^2 = -1$, $\omega = 2\pi f$ is the angular frequency and *n* is an exponent. For n=1, Q models a capacitance with $C=Y_0$ for n=0 and a resistance with $R=Y_0^{-1}$. A special case, the so-called Warburg element, is obtained for n=0.5. This equivalent circuit gives a good description of the impedance data obtained ($\chi^2 = 0.000008$) and allows the values of $Q_1$, $R_{ct}$ and $Q_2$ to be calculated. In this experiment, the value of *n* varied from 0.983 to 0.891, indicating that $Q_1$ could be considered as a capacitance, C [33].

$R_{ct}$ is the most sensitive parameter that responds to the electrode. The semicircle diameter in the Nyquist plot is equal to $R_{ct}$. As shown in Figure 2, $R_{ct}$ decreased remarkably after the PGE was modified with MWCNT–PDDA nanocomposites, indicating that MWCNTs, as conducting bridges, promoted the electron transfer for $[Fe(CN)_6]^{3-/4-}$. In Figure 2 (curve c), an obvious increase is observed for $R_{ct}$ after the negatively charged DNA is adsorbed onto the surface of PDDA–MWCNT/PGE. This increase could be attributed to the negatively charged skeleton of DNA in dsDNA/PDDA–MWCNT film, which blocked the diffusion of $[Fe(CN)_6]^{3-/4-}$ into the film and hindered electron transfer. Meanwhile, it also suggests that DNA was successfully immobilized on the PDDA–MWCNT/PGE.

**"Here Figure 2"**

*3.1. VC-driven MD redox cycling*

In order to detect DNA damage, the oxidation signal of the guanine moiety in the acetate buffer solution containing 0.02 mol $L^{-1}$ NaCl (pH 4.8) and the impedimetric signal of dsDNA/PDDA–MWCNT/PGE in 5.0 mmol $L^{-1}$ $K_3[Fe(CN)_6]/K_4[Fe(CN)_6]$ (1:1) (in 0.1 mol $L^{-1}$ KCl), as a redox probe, were used to measure the changes occurring in the surface-attached DNA while the electrode was being treated.

DNA damage could be characterized from the appearance of the oxidation peaks of the bases from the DNA molecule. The decrease in the oxidation current of guanine moiety ($I_p$), recorded by DPV, was used to determine the extent of the oxidative damage. Figure 3 (curve a in (i)) shows the anodic peak of guanine moiety at 1.02 V (*vs.* Ag/AgCl). The DPV results of the DNA-based biosensor, after incubation (30 min) in 0.01 mmol $L^{-1}$ MD solution without any reducing agent (curve b in Figure 3(i)), showed a decrease in the peak current. This indicates an interaction between MD and the DNA immobilized on the surface of the MWCNT-PDDA/PGE, which leads to the shielding of the guanine, which would otherwise be capable of reacting with MD. The decrease in $I_p$ was attributed to the binding of MD to the electroactive DNA base. The impedimetric results (curve b in Figure 3(ii)) show that the presence of MD led to increased $R_{ct}$, indicating that the interaction between MD and DNA (immobilized on the MWCNT-PDDA/PGE) takes place without DNA degradation and that MD molecules are condensed on the DNA surface, thus increasing the $R_{ct}$ value of the biosensor. **"Here Figure 3"**

In the second stage of this work, the DNA-based biosensor was incubated (30 min) in the MD solution (0.01 mmol $L^{-1}$) in the presence of VC (1.0 mmol $L^{-1}$) in 0.1 mol $L^{-1}$ PBS (pH 7.0) for 30 min under stirring. The DNA-based biosensor was subsequently rinsed with water. Then, the voltammetric and impedimetric responses were obtained in an appropriate supporting electrolyte as described in the above section. The results showed that the $I_p$ value (curve c in Figure 3 (i)) of guanine (from the DNA immobilized on the MWCNT-PDDA/PGE surface) and the $R_{ct}$ value of the biosensor (curve c in Figure 3 (ii)) decreased after the DNA-based biosensor was incubated in the MD solution and VC. These observations indicate that the surface-confined DNA was damaged, because the $R_{ct}$ and the oxidation signal of the DNA bases were decreased. In other words, the diminished negative charge facilitated conversion of the ferri-/ferrocyanide redox couple and led to the lower

accessibility of guanine to the electrode surface; hence, the oxidation signal of guanine moiety decreased. Change in the surface-attached dsDNA, after its incubation in the damaging solution, was indicated by a decrease in the $R_{ct}$ of $K_3[Fe(CN)_6]/K_4[Fe(CN)_6]$ and $I_p$ of the guanine moiety [34]. It may, therefore, be considered that MD is not a DNA-damaging agent, rather, it induces damage to DNA in the presence of VC. It needs be noted that VC alone cannot induce significant changes in the voltammetric and impedimetric parameters either and, thus, does not cause any DNA damage (Figure not shown). As reported in the literature [12,13] and as briefly stated in the Introduction, the reductase specifically reduces quinones into semiquinones ($Q^{\cdot -}$) during the redox cycling event; it is, therefore, a very interesting candidate for serving as a reducing agent to mimic the enzymatic quinone redox cycling in VC. In this regard, it is known that VC can promote quinone redox cycling and a combination of VC and MD generates ROS compounds such as $O_2^{\cdot -}$, $H_2O_2$ and $OH^{\cdot}$. The ROS compounds generated from the redox cycling process induce damage to the surface-confined DNA, which then leads to drastic reductions in both oxidation signals of the DNA bases and the $R_{ct}$ values for the biosensor.

In another experiment, the DNA-based biosensor was allowed to interact with the VC–MD solution plus small amounts of Fenton's catalyst (Fe(III)) for 30 min. The biosensor was subsequently immersed in an appropriate supporting electrolyte, followed by EIS and DPV scanning. As shown in curves d in Figure 3 (i and ii), considerable reductions are observed in $R_{ct}$ and $I_p$ when Fe(III) is added to the damaging solution (VC:MD combination). $H_2O_2$ decomposed into more toxic ROS compounds (hydroxyl and hydroperoxyl radicals) via the simplified Fenton's reactions expressed below [18]:

$$Fe^{3+} + H_2O_2 \longrightarrow Fe^{2+} + {\cdot}OOH + H^+ \quad (1)$$

$$Fe^{2+} + H_2O_2 \longrightarrow Fe^{3+} + {\cdot}OH + OH^- \quad (2)$$

The presence of these strong toxic radicals caused a rapid increase in damage in the surface-confined DNA due to the extreme and indiscriminate reactivity of these radicals [13]. The results are shown as histogram plots in Figure 3 (iii) and (iv).

The results obtained from the Nyquist plot and their model Randles equivalent circuit also confirm the decrease in capacitance at the electrode/electrolyte interface following damage to the DNA and the resulting reduced density of the negative charges (of the phosphate groups) [25,33]. Once the biosensor is exposed to the VC:MD combination in the absence and presence of Fe(III), the capacitance is expected to decrease due to the damage of DNA. The results presented in Figure 3(iv) confirm this damage with the accompanying decrease in capacitance by as much as 100 and 160 nF for the VC:MD combination in the absence and presence of Fe(III), respectively. This decrease is confirmed by the data on reduced $R_{ct}$ values reported previously.

*3.2. NADH-driven MD redox cycling*

In order to understand the performance of the electrochemical DNA-based biosensor in determining the effect of NADH on MD redox cycling, the biosensor was incubated in MD solution (0.010 mmol $L^{-1}$) in the presence of NADH (0.0010 mmol $L^{-1}$) in 0.1 mol $L^{-1}$ PBS (pH 7.0) for 30 min under stirring. The biosensor was subsequently rinsed with water. Then, the voltammetric and impedimetric responses were obtained in an appropriate supporting electrolyte described in the section on Apparatus. The results (curves c in Figure 4(i and ii)) show that the values for both the guanine moiety $I_p$ and biosensor $R_{ct}$ decreased. As shown in Figure 4(iv), the capacitance of the electrode/electrolyte interface also decreased after the biosensor was incubated in the MD solution in the presence of NADH. It may, therefore, be considered MD induced damage to DNA in the presence of NADH. NADH alone led to no significant changes in the voltammetric and impedimetric signals and did not induce any DNA damage (Figure not shown). This result confirms the proposition that free radicals are

produced by MD redox cycling in the presence of NADH as a reducing agent. In addition, the presence of Fe(III) ions as Fenton's catalyst, resulted in a considerable decrease in $I_p$ (the guanine base of DNA immobilized on the MWCNT-PDDA/PGE), $R_{ct}$ and the capacitance of the biosensor. This underlines the role of Fe(III) ions in creating stronger free radicals from the peroxide produced by the redox cycle. The results are shown as histogram plots in Figure 4 (iii) and (iv). **"Here Figure 4"**

*3.3. Electroreduction-driven MD redox cycling*

As the next goal of this study, we investigated the performance of the DNA-based biosensor in determining the effect of electro-reductively activated MD on the MD redox cycling. For this purpose, a potential range covering the electrochemical reduction of MD was employed using constant-potential electrolysis. The biosensor was immersed in PBS (pH 7.0) containing 0.01 mmol $L^{-1}$ MD while the solution was being stirred at 200 rpm, and a negative potential, $E_C$, was applied to the electrode for 15 min. Then, the electrode was washed and the EIS and DPV signals of the electrode were recorded in the relevant supporting electrolytes. The recorded $R_{ct}$ and $I_p$ values were used as a measures of the interactions with the surface-attached DNA during the electrode treatment. Therefore, thirteen potentials were applied ranging from 0.00 to –0.80 V. The results obtained (Figure 5(i and ii)) show that the values of $R_{ct}$ and $I_p$ remained constant up to a potential of –0.20 V (*vs.* Ag/AgCl) beyond which they were reduced. In addition, at a potential of –0.50 V (*vs.* Ag/AgCl), $R_{ct}$ and $I_p$ reached constant values. The data obtained from the investigation of the electroreduction time showed that maximum reductions in $R_{ct}$ and $I_p$ were obtained at 15 min. No significant differences were observed in the values of $R_{ct}$ and $I_p$ after the initial 15 min. Clearly then, the interaction occurs in less than 15 min. In the control DNA, the DNA-based biosensor was immersed in PBS in the absence of MD and negative potentials were applied

to the electrode for 15 min; no significant changes were observed in the values of $R_{ct}$ or $I_p$. **"Here Figure 5"**

Figure 6 shows the Nyquist spectrum and DP voltammograms of the DNA-based biosensor in an electro-reduced MD solution (curves c in Figure 6 (i and ii)) and in an oxygen-saturated electro-reduced MD solution (curves d in Figure 6 (i and ii)). The results show that $R_{ct}$ and $I_p$ exhibited greater decreases after the solution had been saturated with oxygen. It may be concluded that presence of oxygen generated more ROS from the electroreduction-driven MD redox cycling, which then induced further damage to the surface-confined DNA. As shown in curves e in Figure 6 (i and ii), and similar to the previously stated reduction methods (VC:MD and NADH:MD combination), remarkable decreases were observed in $R_{ct}$ and $I_p$ when Fe(III) was added to the damaging solution before electro-reduction. The results are presented as histograms in Figure 6 (iii) and (iv). As shown in Figure 6 (iv), changes in the capacitance of the electrode/electrolyte interface exhibited a trend similar to those of $R_{ct}$ and $I_p$, albeit with a lower intensity. **"Here Figure 6"**

*3.4. Effect of superoxide dismutase (SOD)*

SOD acts as an antioxidant and protects cellular components from being oxidized by ROS. To investigate the role of ROS in the reaction of DNA with MD, the effect of SOD was investigated. The results showed that $R_{ct}$ and $I_p$ did not change after SOD was added to the MD solution in the absence of reducing agents. However, these parameters changed with MD solutions containing VC or NADH (Table 1). Clearly, DNA damage induced by MD plus VC or NADH was inhibited by SOD. It may be argued that SOD decomposed the reactive species generated by MD plus VC or NADH, indicating that the reactive species generated from these combinations were ROS. **"Here Table 1"**

## 4. Conclusions

This study investigated the applicability of electrochemical DNA-based biosensors to redox cycling. MD molecules, which are a kind of quinone known to undergo redox cycling, were chosen for this purpose. Results confirmed that EIS and DPV are good alternative techniques to monitor radicals generated as a result of quinone redox cycling. A one-electron reduction of quinone was accomplished by VC, NADH, and electroreduction to initiate the redox cycling, and change in the $R_{ct}$, C and $I_p$ of the biosensor were used as indicators of the extent of radical generation. The free-radical scavenging capacity of SOD and the reducing power of different reagents for the reduction of quinones were investigated using the DNA-based biosensors. It was found that these biosensors are promising and might be a major step toward monitoring chemical reactions involving radicals. The utility of the electrochemical DNA-based biosensors to monitor chain reactions involving free radicals is not only cost-effective but provides for rapid detection. The proposed electroanalytical method is experimentally convenient, sensitive, selective and rapid and can be used with small amounts of materials.



## Acknowledgements

The authors wish to thank the Research Council of Isfahan University of Technology (IUT), the Center of Excellence in Sensor and Green Chemistry and the Iranian Nanotechnology Initiative Council for their support.

## References

[1] M.T. Smith, C.G. Evans, H. Thor, S. Orrenius, Quinone-induced oxidative injury to cells and tissues, in: H. Sies (Ed.), Oxidative Stress, Academic Press., London, 1985, pp. 91–96.

[2] T.W. Gant, R.D.N. Rao, R.P. Mason, G.M. Cohen, Redox cycling and sulphydryl arylation; their relative importance in the mechanism of quinone cytotoxicity to isolated hepatocytes, Chem. Biol. Interact. 65 (1988) 157–173.

[3] G.K Dryhurst, K. Kadish, F. Scheller, Biological Electrochemistry, in: T.P. Singer (Ed.), Biological Oxidations, Academic Press., New York, 1982, p. 533.

[4] M. Uchimiya, A.T. Stone, Reversible redox chemistry of quinones: impact on biogeochemical cycles, Chemosphere 77 (2009) 451–458.

[5] F. Guillen, M.J. Martínez, C. Muñoz, A.T. Martínez, Quinone redox cycling in the ligninolytic fungus Pleurotus eryngii leading to extracellular production of superoxide anion radical, Arch Biochem. Biophys. 339 (1997) 190–199.

[6] A. Rybina, B. Thaler, R. Krämer, D.-P. Herten, Monitoring hydroquinone-quinone redox cycling by single molecule fluorescence spectroscopy, Phys. Chem. Chem. Phys. 16 (2014) 19550–19555.

[7] P.R. Rich, Electron and proton transfers in chemical and biological quinone systems, Faraday Discuss. Chem. Soc. 74 (1982) 349–364.

[8] K. Reybier, P. Perio, G. Ferry, J. Bouajila, P. Delagrange, J.A. Boutin, F. Nepveu, Insights into the redox cycle of human quinone reductase 2, Free Radic. Res. 45 (2011) 1184–1195.

[9] D. Bao, S. Ramu, A. Contreras, S. Upadhyayula, J.M. Vasquez, G. Beran V.I. Vullev, Electrochemical reduction of quinones: interfacing experiment and theory for defining effective radii of redox moieties, J. Phys. Chem. B 114 (2010) 14467–14479.

[10] P.L. Gutierrez, The metabolism of quinone containing alkylating agents: Free radical production and measurement, Front Biosci. 5 (2000) D629–638.

[11] M.V.C. Nguyen, B. Lardy, F. Rousset, F. Hazane-Puch, L. Zhang, C. Trocmé, L. Serrander, K.H. Krause, F. Morel, Quinone compounds regulate the level of ROS production by the NADPH oxidase Nox4, Biochem. Pharmacol. 85 (2013) 1644–1654.

[12] A.R. Bonilla-Porras, M. Jimenez-Del-Rio, C. Velez-Pardo, Vitamin K3 and vitamin C alone or in combination induced apoptosis in leukemia cells by a similar oxidative stress signaling mechanism, Cancer Cell Int. 19 (2011) 11–18.

[13] Y. Li, T. Zhu, J. Zhao, B. Xu, Interactive enhancements of ascorbic acid and iron in hydroxyl radical generation in quinone redox cycling, Environ. Sci. Technol. 46 (2012) 10302–10309.

[14] D. Ross, H. Thor, S. Orrenius, P. Moldeus, Interaction of menadione (2-methyl-1,4-naphthoquinone) with glutathione, Chem. Biol. Interact. 55 (1985) 177–184.

[15] Y. Shang, C. Chen, Y. Li, J. Zhao, T. Zhu, Hydroxyl radical generation mechanism during the redox cycling process of 1,4-naphthoquinone, Environ. Sci. Technol. 46 (2012) 2935–2942.

[16] Z. Wang, E.R. Chandrasena, Y. Yuan, K.W. Peng, R.B. Breemen, G.R.J. Thatcher, J.L. Bolton, Redox cycling of catechol estrogens generating apurinic/apyrimidinic sites and 8-oxo-deoxyguanosine via reactive oxygen species differentiates equine and human estrogens, Chem. Res. Toxicol. 23 (2010) 1365–1373.

[17] M.S. Cooke, M.D. Evans, M. Dizdaroglu, J. Lunec, Oxidative DNA damage: mechanisms, mutation, and disease, FASEB J. 17 (2003) 1195–1214.

[18] W.A. Spencer, M.V. Vadhanam, J. Jeyabalan, R.C. Gupta, Oxidative DNA damage following microsome/Cu(II)-mediated activation of the estrogens, 17β-estradiol,

equilenin, and equilin: role of reactive oxygen species, Chem. Res. Toxicol. 25 (2012) 305–314.

[19] A.A. Ensafi, P. Nasr-Esfahani, E. Heydari-Bafrooei, B. Rezaei, Determination of atropine sulfate using a novel sensitive dna–biosensor based electrochemical interaction on modified pencil graphite electrode, Talanta 131 (2015) 149–155.

[20] M. Chen, H. Xiong, X. Zhang, H. Gu, S. Wang, Electrochemical biosensors for the monitoring of DNA damage induced by ferric ions mediated oxidation of dopamine, Electrochem. Commun. 28 (2013) 91–94.

[21] A.A. Ensafi, H.R. Jamei, E. Heydari-Bafrooei, B. Rezaei, development of a voltammetric procedure based on dna interaction for sensitive monitoring of chrysoidine, a banned dye, in foods and textile effluent, Sens. Actuators B 202 (2014) 224–231.

[22] Y. Wang, H. Xiong, X. Zhang, S. Wang, Electrochemical biosensors for the detection of oxidative DNA damage induced by Fenton reagents in ionic liquid, Sens. Actuators B 161 (2012) 274–278.

[23] M. Chen, H. Xiong, W. Wen, X. Zhang, H. Gu, S. Wang, Electrochemical biosensors for the assay of DNA damage initiated by ferric ions catalyzed oxidation of dopamine in room temperature ionic liquid, Electrochim. Acta 114 (2013) 265–270.

[24] A.A. Ensafi, N. Kazemnadi, M. Amini, B. Rezaei, Impedimetric DNA-biosensor for the study of dopamine induces dna damage and investigation of inhibitory and repair effects of some antioxidants, Bioelectrochemistry 104 (2015) 71–78.

[25] Y. Kuzin, A. Porfireva, V. Stepanova, V. Evtugyn, I. Stoikov, G. Evtugyn, T. Hianik, Impedimetric detection of DNA damage with the sensor based on silver nanoparticles and neutral red, Electroanalysis 27 (2015) 2800–2808.

[26] H. Karadeniz, B. Gulmez, F. Sahinci, A. Erdem, G.I. Kaya, N. Unver, B. Kivcak, M. Ozsoz, Disposable electrochemical biosensor for the detection of the interaction between

DNA and lycorine based on guanine and adenine signals, J. Pharm. Biomed. Anal. 33 (2003) 295-302.

[27] Z. Chang, M. Chen, H. Fan, K. Zhao, S. Zhuang, P. He, Y. Fang, Multilayer membranes via layer-by-layer deposition of PDDA and DNA with Au nanoparticles tags for DNA biosensing, Electrochim. Acta 53 (2008) 2939–2945.

[28] R.L. McCreery, Carbon electrodes: Structural Effects On Electron Transfer Kinetics, in: A.J. Bard (Ed.), Electroanalytical Chemistry, Marcel Dekker, New York, 1991, pp. 221–374.

[29] M. Souiri, N. Blel, D. Sboui, L. Mhamdi, T. Epalle, R. Mzoughi, S. Riffard, A. Othmane, AFM, CLSM and EIS characterization of the immobilization of antibodies on indium–tin oxide electrode and their capture of Legionella pneumophila, Talanta 118 (2014) 224–230.

[30] C.Z. Li, Y. Liu, J.H.T. Luong, Impedance sensing of DNA binding drugs using gold substrates modified with gold nanoparticles, Anal. Chem. 77 (2005) 478–485.

[31] O.A. Sadik, H. Xu, E. Gheorghiu, D. Andreescu, C. Balut, M. Gheorghiu, D. Bratu, Differential impedance spectroscopy for monitoring protein immobilization and antibody-antigen reactions, Anal. Chem. 74 (2002) 3142–3150.

[32] S.M. Park, J.S. Yoo, Peer reviewed: electrochemical impedance spectroscopy for better electrochemical measurements, Anal. Chem. 75 (2003) 455A–461A.

[33] C. Tlili, N.J. Jaffrezic-Renault, C. Martelet, H. Korri-Youssoufi, Direct electrochemical probing of DNA hybridization on oligonucleotide-functionalized polypyrrole, Mater. Sci. Eng. C, 28 (2008) 848–854.

[34] J. Labuda, R. Ovadekova, J. Galandova, DNA-based biosensor for the detection of strong damage to DNA by the quinozaline derivative as a potential anticancer drug, Microchim. Acta 164 (2009) 371–377.

**Table 1.** Inhibitory effect of SOD on the DNA damage after 30 min incubation in different reagents.

| Reagents | $R_{ct}$[a] (Ω) | | $I_p$[a] (μA) | |
|---|---|---|---|---|
| | Without SOD | 0.5 mg $mL^{-1}$ SOD | Without SOD | 0.5 mg $mL^{-1}$ SOD |
| 0.1 mol $L^{-1}$ PBS | 695 ± 21 | 691 ± 18 | 23.8 ± 0.9 | 23.5 ± 1.0 |
| 0.1 mol $L^{-1}$ PBS containing 0.01 mmol $L^{-1}$ MD | 724 ± 25 | 732 ± 20 | 17.1 ± 0.6 | 17.4 ± 0.6 |
| 0.1 mol $L^{-1}$ PBS containing 0.01 mmol $L^{-1}$ MD + 1.0 mmol $L^{-1}$ VC | 533 ± 23 | 702 ± 29 | 15.2 ± 0.7 | 17.8 ± 0.8 |
| 0.1 mol $L^{-1}$ PBS containing 0.01 mmol $L^{-1}$ MD + 1.0 mmol $L^{-1}$ VC + Fe(III) | 482 ± 18 | 712 ± 31 | 12.4 ± 0.6 | 17.1 ± 0.8 |
| 0.1 mol $L^{-1}$ PBS containing 0.01 mmol $L^{-1}$ MD + 0.001mmol $L^{-1}$ NADH | 580 ± 20 | 700 ± 26 | 11.9 ± 0.5 | 16.8 ± 0.9 |
| 0.1 mol $L^{-1}$ PBS containing 0.01 mmol $L^{-1}$ MD + 0.001 mmol $L^{-1}$ NADH + Fe(III) | 397 ± 13 | 695 ± 23 | 8.4 ± 0.4 | 17.9 ± 0.8 |
| 0.1 mol $L^{-1}$ PBS containing 0.01 mmol $L^{-1}$ MD and applying –0.5 V | 552 ± 17 | 712 ± 25 | 13.7 ± 0.8 | 17.0 ± 0.8 |
| 0.1 mol $L^{-1}$ PBS containing 0.01 mmol $L^{-1}$ MD + $O_2$ and applying –0.5 V | 524 ± 19 | 709 ± 22 | 12.8 ± 0.5 | 17.5 ± 0.7 |
| 0.1 mol $L^{-1}$ PBS containing 0.01 mmol $L^{-1}$ MD + Fe(III) and applying –0.5 V | 424 ± 19 | 714 ± 26 | 10.4 ± 0.4 | 17.2 ± 0.9 |

[a] data expressed as the mean ± the standard deviation (n=3)

**Legends for the figures**

**Figure 1.** SEM images of (A) bare PGE, (B) MWCNT–PDDA/PGE, and (C) DNA/MWCNT–PDDA/PGE.

**Figure 2.** (i) Impedance spectra of a): bare PGE; b): MWCNT–PDDA/PGE, and c): DNA/MWCNT–PDDA/PGE in 5.0 mmol $L^{-1}$ $[Fe(CN)_6^{3-/4-}]$ containing 0.10 mol $L^{-1}$ KCl. Inset: Equivalent circuit for fitting the plots. $R_s$: electrolyte solution resistance; $R_{ct}$: interfacial electron transfer resistance; $Q_1$: space charge capacitance between electrode and solution; $Z_W$: Warburg impedance resulting from the diffusion of ions.

**Figure 3.** (i) DP voltammograms of guanine moiety in the acetate buffer solution containing 0.02 mol $L^{-1}$ NaCl (pH 4.8) at the surface of DNA/MWCNT–PDDA/PGE; and (ii) Impedance spectra of DNA/MWCNT–PDDA/PGE in 5.0 mmol $L^{-1}$ $[Fe(CN)_6^{3-/4-}]$ containing 0.1 mol $L^{-1}$ KCl. DNA/MWCNT–PDDA/PGE was incubated in (a) 0.1 mol $L^{-1}$ PBS (pH 7.0), (b) 0.1 mol $L^{-1}$ PBS (pH 7.0) containing 0.010 mmol $L^{-1}$ MD, (c) 0.1 mol $L^{-1}$ PBS (pH 7.0) containing 0.010 mmol $L^{-1}$ MD in the presence of 1.0 mmol $L^{-1}$ VC, and (d) 0.1 mol $L^{-1}$ PBS (pH 7.0) containing 0.010 mmol $L^{-1}$ MD in the presence of 1.0 mmol $L^{-1}$ VC and small amount of Fe(III) with stirring time of 30 min. (iii) Dependence of Ip and (iv) C and $R_{ct}$ on MD and VC, as histogram.

**Figure 4.** (i) DP voltammograms of guanine moiety in the acetate buffer solution containing 0.02 mol $L^{-1}$ NaCl (pH 4.8); and (ii) Impedance spectra of DNA/MWCNT–PDDA/PGE in 5.0 mmol $L^{-1}$ $[Fe(CN)_6^{3-/4-}]$ containing 0.1 mol $L^{-1}$ KCl at the surface of DNA/MWCNT–PDDA/PGE. DNA/MWCNT–PDDA/PGE was incubated in (a) 0.1 mol $L^{-1}$ PBS (pH 7.0), (b) 0.1 mol $L^{-1}$ PBS (pH 7.0) containing 0.010 mmol $L^{-1}$ MD, (c) 0.1 mol $L^{-1}$ PBS (pH 7.0) containing 0.010 mmol $L^{-1}$ MD in the presence of 0.001 mmol $L^{-1}$ NADH, and (d) 0.1 mol

$L^{-1}$ PBS (pH 7.0) containing 0.010 mmol $L^{-1}$ MD in the presence of 0.001 mmol $L^{-1}$ NADH and small amount of Fe(III) with stirring time of 30 min. (iii) Dependence of $I_p$, and (iv) C and $R_{ct}$ on MD and NADH, as histogram.

**Figure 5.** Effect of the reduction potential on (i) $R_{ct}$ of the biosensor, and (ii) $I_p$ of guanine moiety after immersion of DNA/MWCNT–PDDA/PGE in 0.1 mol $L^{-1}$ PBS (pH 7.0) containing 0.010 mmol $L^{-1}$ MD.

**Figure 6.** (i) DP voltammograms of guanine moiety in the acetate buffer solution containing 0.02 mol $L^{-1}$ NaCl (pH 4.8), and (ii) Impedance spectra of DNA/MWCNT–PDDA/PGE in 5.0 mmol $L^{-1}$ $[Fe(CN)_6^{3-/4-}]$ containing 0.1 mol $L^{-1}$ KCl at the surface of DNA/MWCNT–PDDA/PGE. The DNA-based biosensor was incubated in: (a) 0.1 mol $L^{-1}$ PBS (pH 7.0), (b) 0.1 mol $L^{-1}$ PBS (pH 7.0) containing 0.010 mmol $L^{-1}$ MD, (c) 0.1 mol $L^{-1}$ PBS (pH 7.0) containing 0.010 mmol $L^{-1}$ MD, (d) oxygen-saturated solution of 0.1 mol $L^{-1}$ PBS (pH 7.0) containing 0.010 mmol $L^{-1}$ MD, and (e) 0.1 mol $L^{-1}$ PBS (pH 7.0) containing 0.010 mmol $L^{-1}$ MD in the presence of small amount of Fe(III), with stirring time of 15 min. (iii) Dependence of $I_p$ and (iv) C and $R_{ct}$ on the electroreductived MD, as a histogram (V is voltage).

**Scheme 1.** General quinone redox cycling.

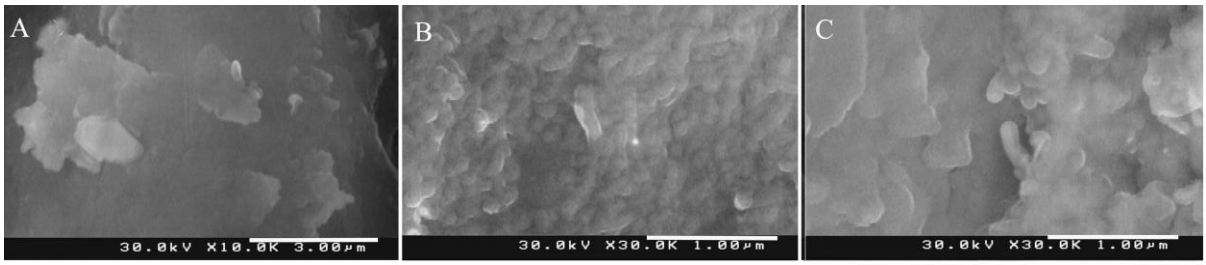


Fig. 1

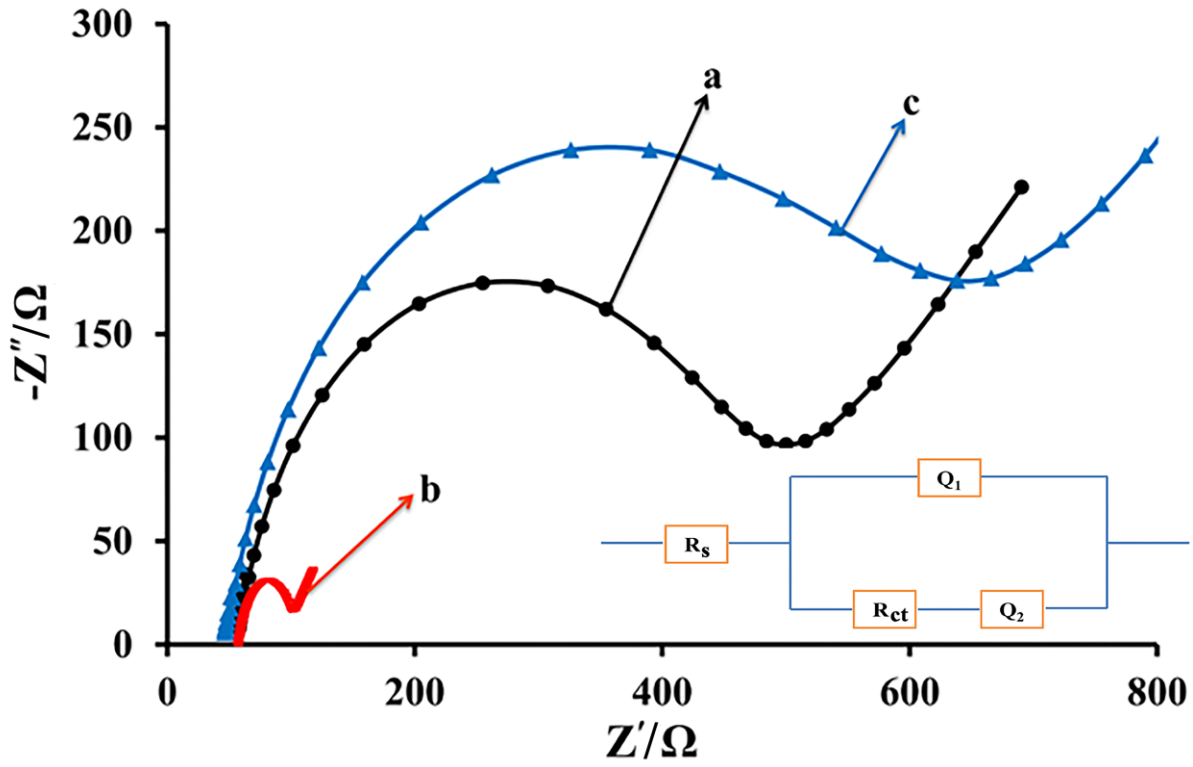


Fig. 2

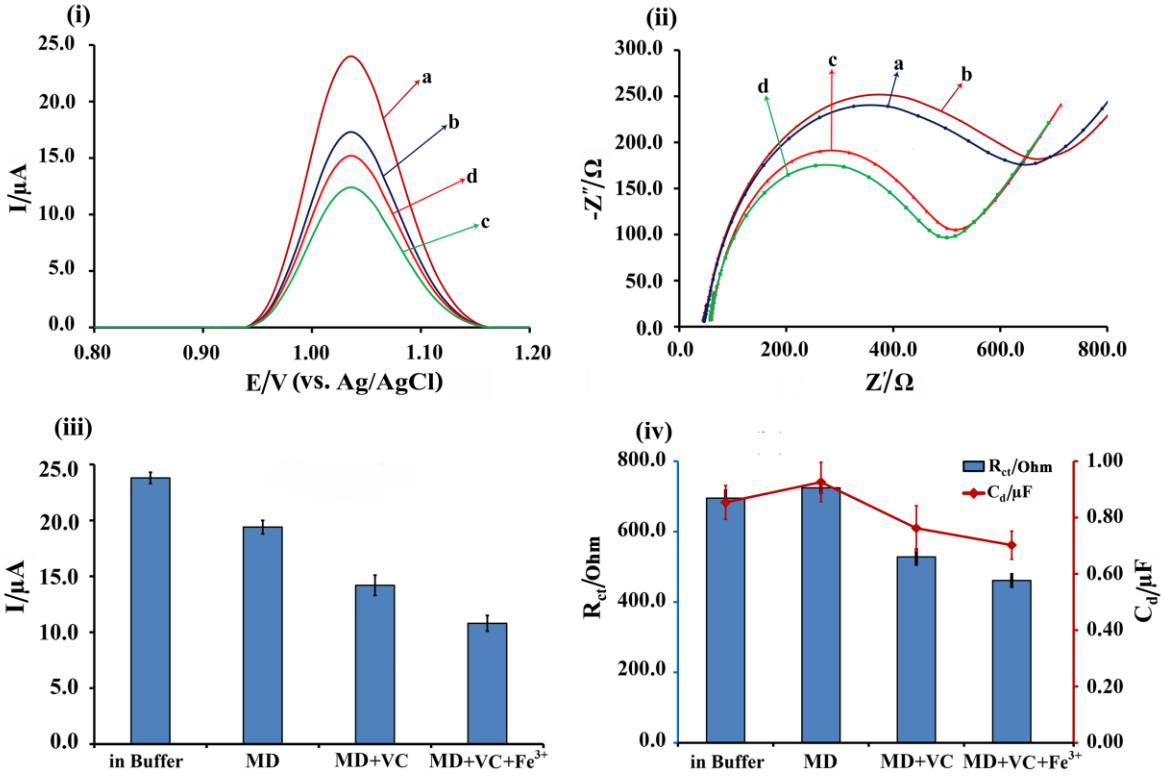


Fig. 3

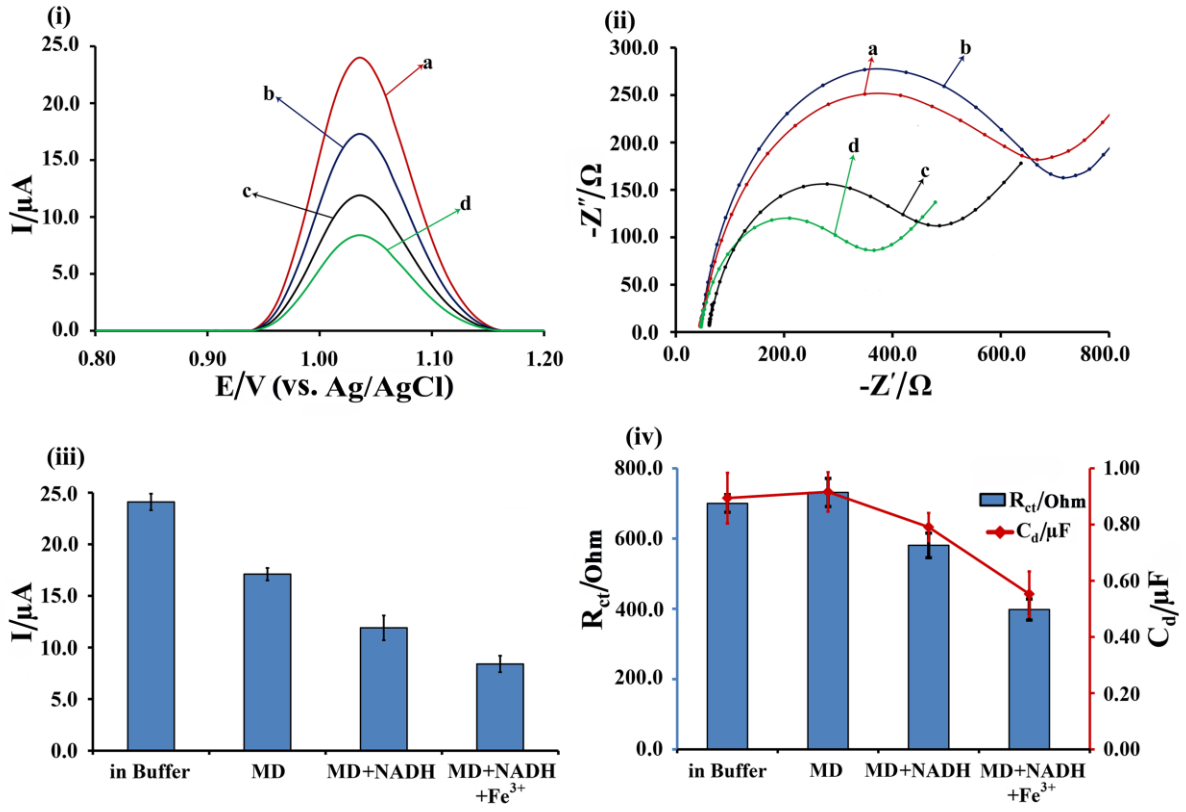


Fig. 4

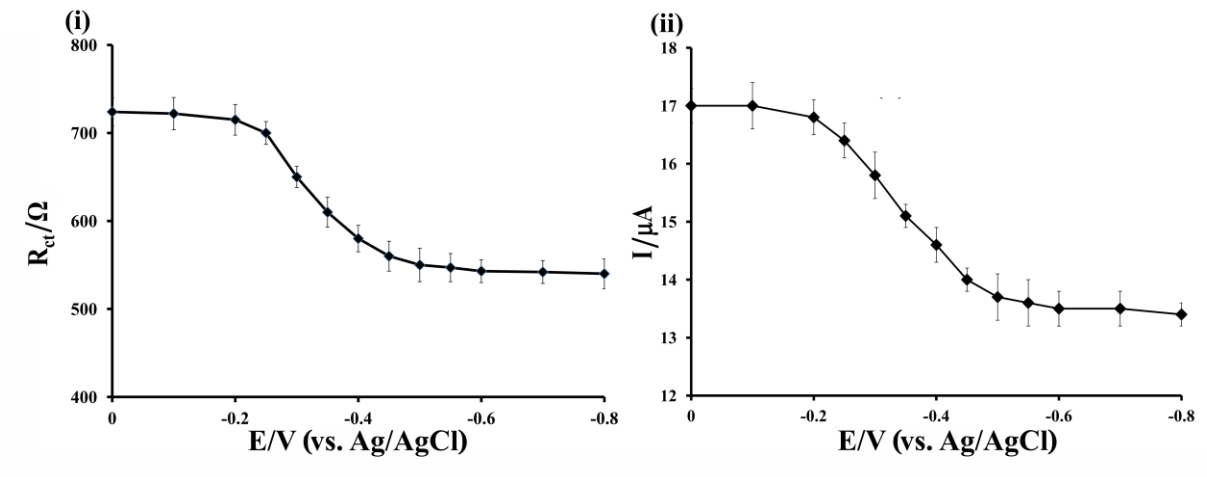


Fig. 5

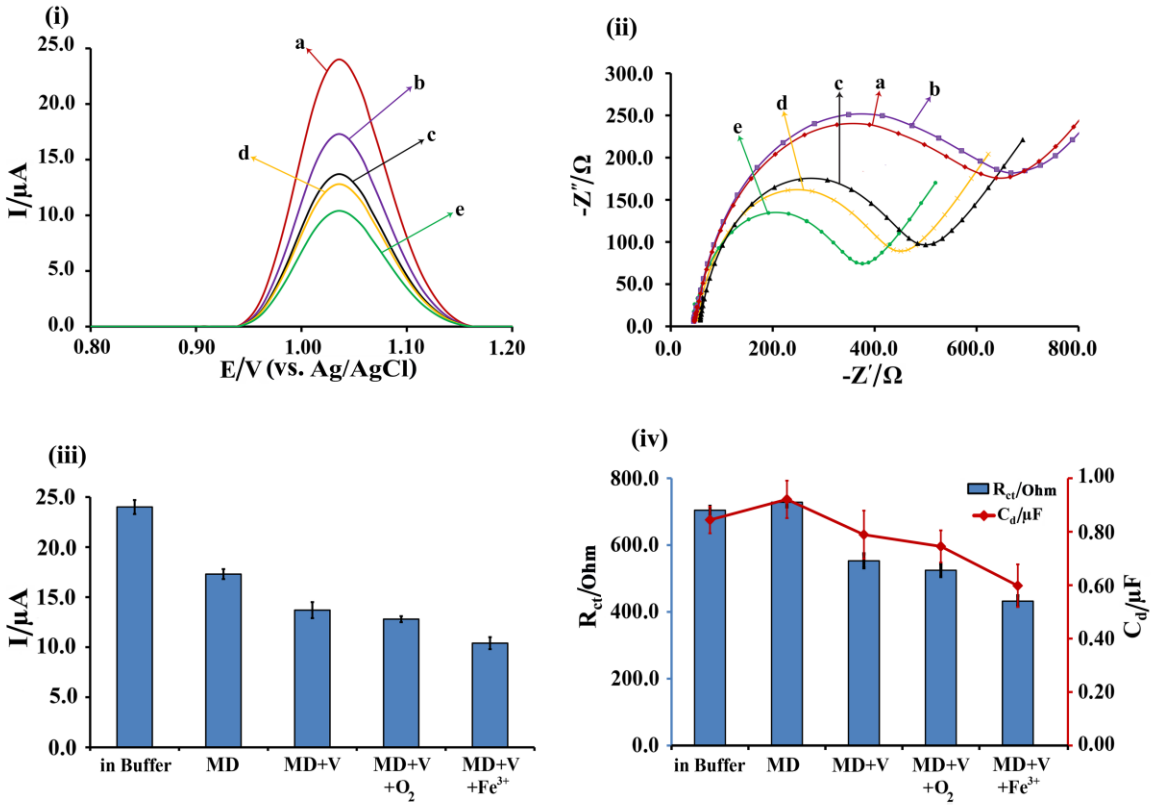


Fig. 6

Scheme 1

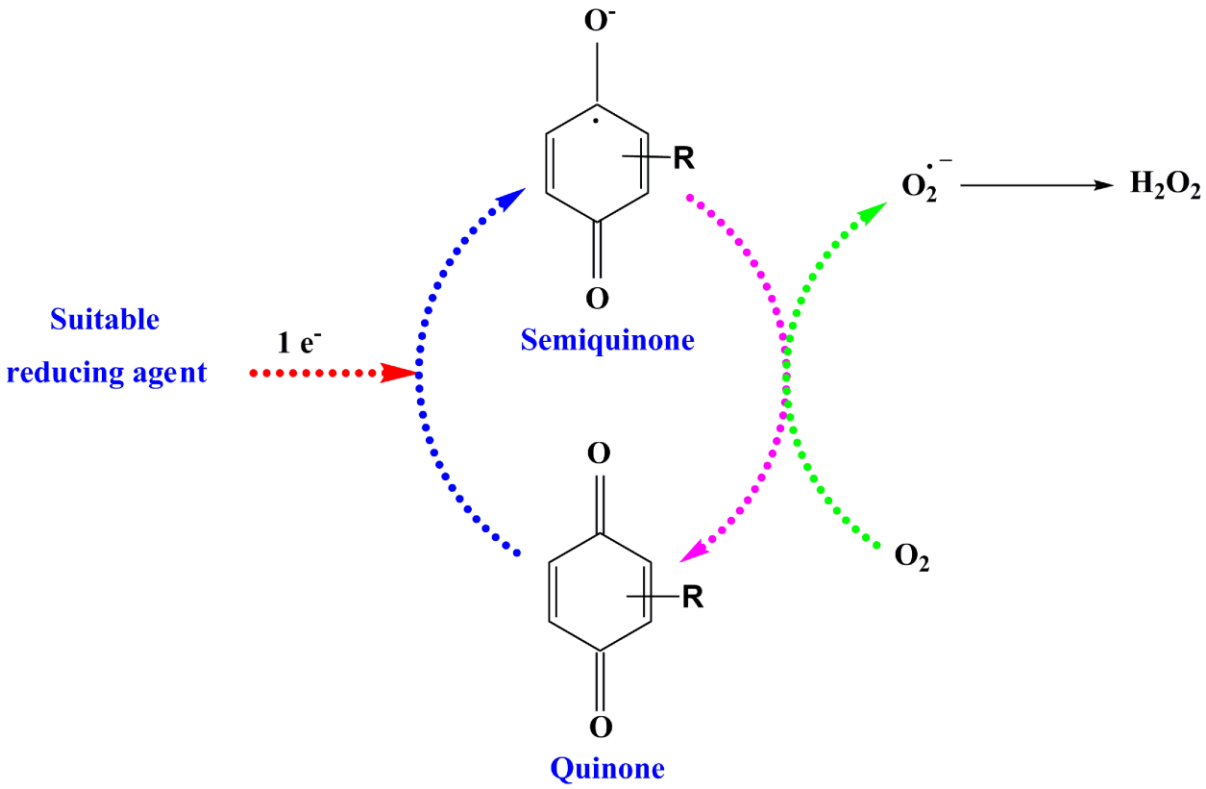

Graphical abstract

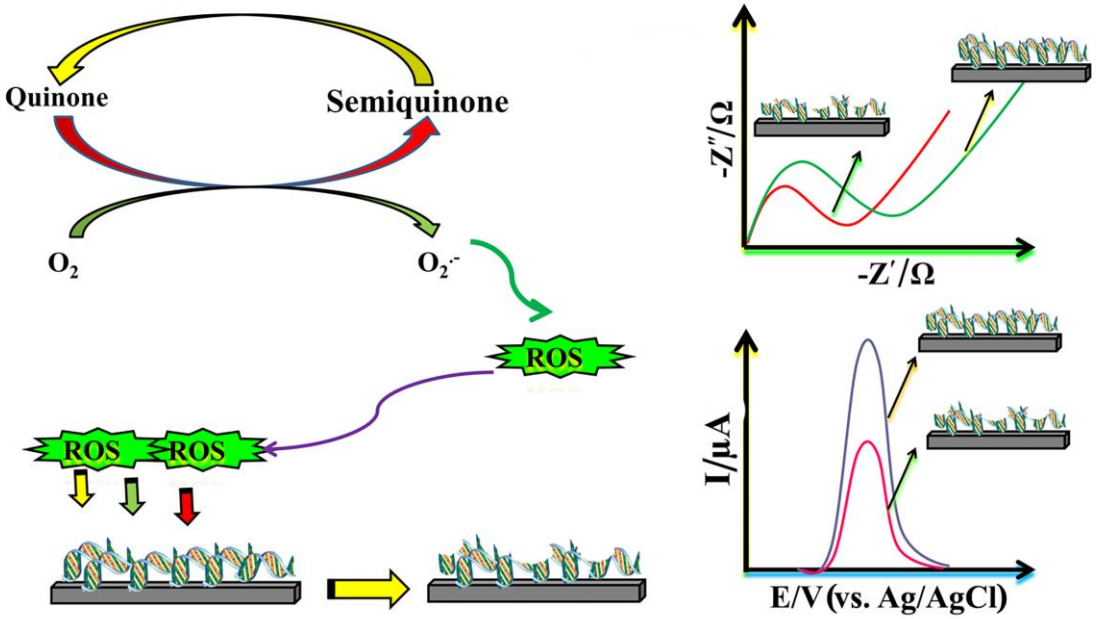

Highlights

- A DNA-biosensor was used to investigate biological and chemical redox cycling reactions.
- Differential pulse voltammetry and electrochemical impedance spectroscopy were used.
- 2-Methyl-1,4-naphthoquinone was employed as a model to study the redox cycling.
- Charge transfer resistance and guanine oxidation signal were used as indicators.
- There is a direct relationship between free radical production and DNA damage.